Thermal desorption of molecular oxygen from SnO_2 (110) surface: Insights from first-principles calculations

Viacheslav Golovanov[1,2], Viktoria Golovanova[1], Tapio T. Rantala[2]

[1]*South-Ukrainian University, Staroportofrankovskaya Str., 26, 65008, Odessa, Ukraine*
[2]*Tampere University of Technology, P.O. Box 692, FI-33101 Tampere, Finland*

Abstract

First-principles calculations based on density functional theory in the generalized gradient approximation, together with pseudopotentials and plane-wave basis set, have been used to investigate the desorption pathways of molecular oxygen species adsorbed on the SnO_2 (110) surface. The energetics of the thermodynamically favored precursors is studied in dependence of different amount of surface charge provided either by surface defects or by donor-type impurities from the near-surface region. The resonant desorption modes of O_2 molecules are examined in the framework of the *ab initio* atomic thermodynamics and the relationship of these results to experimental observations is discussed.

1. Introduction

Tin dioxide (SnO_2) has been recognized as an attractive material with excellent optical properties, chemical durability, and transparent conductivity [1]. One crucial aspect governing the chemical behavior of SnO_2 is the chemistry associated with oxygen species adsorbed on the thermodynamically most stable (110) surface. The studies based on density functional theory (DFT) indicate that electronic charge transfer to the adsorbates is required to chemisorb oxygen atoms and molecules on the stoichiometric SnO_2 (110) surface [2]. The stabilization of neutral oxygen species is endothermic. For this reason, most of the theoretical calculations that deal with the interaction $SnO_2 \cdots O_2$ have been performed on the reduced (110) surface with bridging (O_{br}) oxygen vacancies [2-6]. It is generally accepted that O_2 adsorbs at O_{br} vacancy sites and acquires negative charge donated by such surface defects. At elevated temperatures oxygen molecules dissociate to fill O_{br} vacancies and form adsorbed oxygen monoatoms at adjacent five-fold coordinated tin sites (Sn_{5c}) on the SnO_2 (110) surface [3].

It should be noted however that the direct scanning tunneling microscopy (STM) observations on the TiO_2 (110) surface which is isostructural with the SnO_2 surface are at variance with these previously proposed models that are based on O_{br} vacancies as the main charge donors [7]. Lira *et al* [8] estimated that more than 90% of the electronic charge withdrawn by the oxygen adsorbates stems from charge donors in the near-surface region. Besides, STM images reveal that O_2 molecules are found on top of Sn_{5c} atoms that constitute troughs along the [001] direction. Such conclusions correlate with temperature-programmed desorption (TPD) experiments, indicating that the full O_2 coverage at a low temperature (120 K) would be approximately three times the surface vacancy population [9]. The authors inferred that adsorbed O_2 molecules may exist either in weakly (below 200 K) or strongly (above 400 K) bound states. The corresponding ionosorption channels for molecular oxygen can be therefore associated with Sn_{5c} troughs and O_{br} vacancies, respectively.

In the chemisorbed-precursor mechanism the incident oxygen molecule initially adsorbs intact and the subsequent interplay between the thermally driven kinetics and the lack of surface electronic charge determines the pathways for O_2 desorption, chemisorption or dissociation.

Although the excess charge can be donated by the various donor-type defects, the most of the DFT studies were performed on the reduced SnO_2 (110) surface, where O_2 adsorption is mediated by the presence of surface O_{br} vacancies. The role of subsurface defects in providing an excess electrons for the $SnO_2 \cdots O_2$ interaction is still unsettled today.

Earlier we have investigated computationally the effects of surplus electrons on the oxidized SnO_2 (110) surface with molecular oxygen adsorbed along the Sn_{5c} rows [10]. Now we compare the surface energetics of these superoxide molecules in conditions where an additional charge is generated by the presence of surface O_{br} vacancies or extrinsic donor-type defects from the near-surface regions.

In the meantime, the oxygen species adsorbed at SnO_2 surface have only been studied in the zero temperature approximation, i.e., by neglecting vibrational and entropy contributions of defect formation. In principle, the parameters of desorption channels for adsorbed O_2 molecule are significantly temperature dependent. In the present paper we examine the effects of the adsorbate motion on the thermally activated bond breaking and judge the calculated vibrational bond-stretching modes by correspondence with the available experimental evidences. The study of O_2 molecules weakly bound along the rows of five-fold coordinated surface tin atoms, which likely are precursors to desorbed gas phase O_2 molecules, allows us to better understand the sequence of elementary steps involved in thermally stimulated desorption of molecular oxygen from the SnO_2 surface.

2. Models and Methods

A unit cell Sn_4O_8 is chosen for modeling of the (110) crystal surface instead of the conventional primitive cell Sn_2O_4 with different orientation. The computational supercell $(Sn_4O_8)_{10}$ is a 2×5×1 multiple of the chosen unit cell. The surface of SnO_2 is therefore represented by three-dimensional periodic slab, consisting of five $O(Sn_2O_2)O$ layers periodic in the [001] and $[1\bar{1}0]$ directions, but finite in the [110] direction. All surfaces are modeled with a vacuum thickness exceeding 12 Å between the slabs. Test calculations were performed with supercell of $(Sn_4O_8)_{20}$, which is a 2×5×2 multiple of the chosen unit cell. No appreciable differences in relaxed surface geometry and binding energy values have been found in simulations where a larger empty space and supercell were used. The middle layer is kept fixed in bulk geometry while all other atoms relax in geometry optimization. Adsorption was allowed on only one of the two sides of the slab used to construct the SnO_2 (110) surface. The calculated coverage of O_2 on the surface is one molecule per supercell, which corresponds to 0.4 of a monolayer. The binding energy of O_2 adsorbate (E_b) is estimated as total energy difference of the supercells with O_2 molecule adsorbed on the surface and O_2 molecule located in the vacuum region of the supercell far from the surface.

The calculations are based on the plane wave basis set with pseudopotential concept as implemented in CASTEP code [11]. The utilizing of ultrasoft pseudopotentials [12] enables to limit considerably the plane wave basis set to cutoff of 400 eV. Oxygen atoms are described by six valence electrons and tin atoms by four plus the corresponding pseudopotential ion cores. Electronic exchange and correlation are included by the Perdew-Burke-Ernzerhof (PBE) generalized-gradient approximation (GGA) allowing possible spin polarization [13]. The Brillouin zone is sampled with 3×1×3 mesh of Monkhorst-Pack special k points. In separate test calculations, the number of irreducible k-points was increased up to 6 (2×2×3 mesh), which does not alter the obtained results. For charged systems, the negative charge of the unit cell is balanced by using constant background positive charge density. The Bader charge analysis has been carried out by means of the VASP package [14] based on the projector augmented wave

method [15] with cutoff set to 700 eV. The VASP software allows efficient use of hybrid PBE0 functional, which reproduces the experimental band gap of 3.6 eV. In several complementary calculations, the PBE0 functional has been used against the GGA-PBE scheme in order to check the effect of the band gap underestimation on the reliability of the calculated adsorption energies. The calculated equilibrium lattice constants for bulk SnO_2 are a=4.83 Å, c=3.23 Å for PBE and a=4.75 Å, c=3.18 Å for PBE0.

In the transition level calculations, the O_2 molecules adsorbed on the SnO_2 surface were treated like surface defects in the same framework successfully used for bulk defects in semiconductors [16]. Similarly, the formation energy (E_f) of an oxygen molecule in charge state q adsorbed on the SnO_2 is defined as:

$$E_f = [E^{tot}(SnO_2{+}O_2,q) - E^{tot}(SnO_2)] + \mu(O_2) + q\varepsilon_F, \quad (1)$$

where $E^{tot}(SnO_2{+}O_2,q)$ and $E^{tot}(SnO_2)$ represent the total energies of the slab with adsorbed O_2 molecule in the charge state q, and that of a pristine slab in the same supercell. We consider that the surface of a slab is in equilibrium with an oxygen reservoir characterized by the chemical potential of oxygen $\mu(O_2)$, which we approximate with the total energy of one O_2 molecule in the vacuum. In order to change the charge state of the defect, electrons are exchanged with the Fermi level ε_F, which in semiconductors is referenced to the valence-band maximum and ranges over the band gap from the valence band maximum (E_V) up to the conduction band minimum (E_C). The Fermi energy values for which the occupation number of an adsorbed O_2 state in the energy gap changes from n to $n + 1$ are given by the Fermi energy position where the formation energies of the n and $n + 1$ charge-states of the O_2 are equal. Thus, electronic levels induced by the adsorbed O_2 molecule in the SnO_2 band gap can be investigated by calculating the $\varepsilon^{n/n+1}[O_2]$ levels. The potential alignment and finite-size correction were included according to scheme proposed in [17].

3. Results and Discussion

3.1. Origin of electronic charge and binding energy

The schematic representation of the oxygen molecules adsorbed at bridging oxygen vacancy and neighboring Sn_{5c} sites are shown in Figure 1, and they are similar to those reported in other first-principles calculations performed on rutile (110) surfaces of SnO_2 and TiO_2 [2-5,18-24]. At O_{br} vacancy the molecular oxygen adsorbs in peroxo form (O_2^{2-}) (Fig. 1(a,b)) and is bound onto the SnO_2 surface strongly enough so that it may only desorb after activation by thermal energy at temperatures higher than 400 K. Lira *et al* [8] propose that an impinging O_2 molecule dissociates if it directly hits the O_{br} vacancy site. The intermediate structure, in which O_2 is located halfway between the vacancy and the Sn_{5c} sites, is presented in Figure 1(c). For studies of the thermally stimulated O_2 desorption pathways however the less stable conformations associated with Sn_{5c} sites (Fig. 1(d-f)) are the most promising.

We focus first on the ionosorbed oxygen molecule bridging two Sn_{5c} atoms and lying parallel to the surface along the [001] direction (Fig. 1(d)). The plausibility of this configuration has been revealed in fast-scanning STM observations [25]. The calculated bonding and electronic structure parameters of O_2 adsorbate are compared in Table 1 for the following molecule-surface systems: i) the supercell, where one to six lattice oxygen atoms are substituted by the fluorine dopants (F_O), ii) the supercell with one to three O_{br} vacancies, iii) the supercell, where F_O and O_{br} vacancy are presented jointly, and iv) the supercell, where additional electrons are provided using the model with constant background positive charge density. The binding energy of oxygen molecule and SnO_2 slab with one O_{br} vacancy (0.43 eV) or one surplus electron (0.41

eV) corroborates results reported previously by Oviedo *et al* [2]. It can be seen however that interaction of adsorbed O_2 with SnO_2 surface strongly depends on the origin and amount of the surface excess charge.

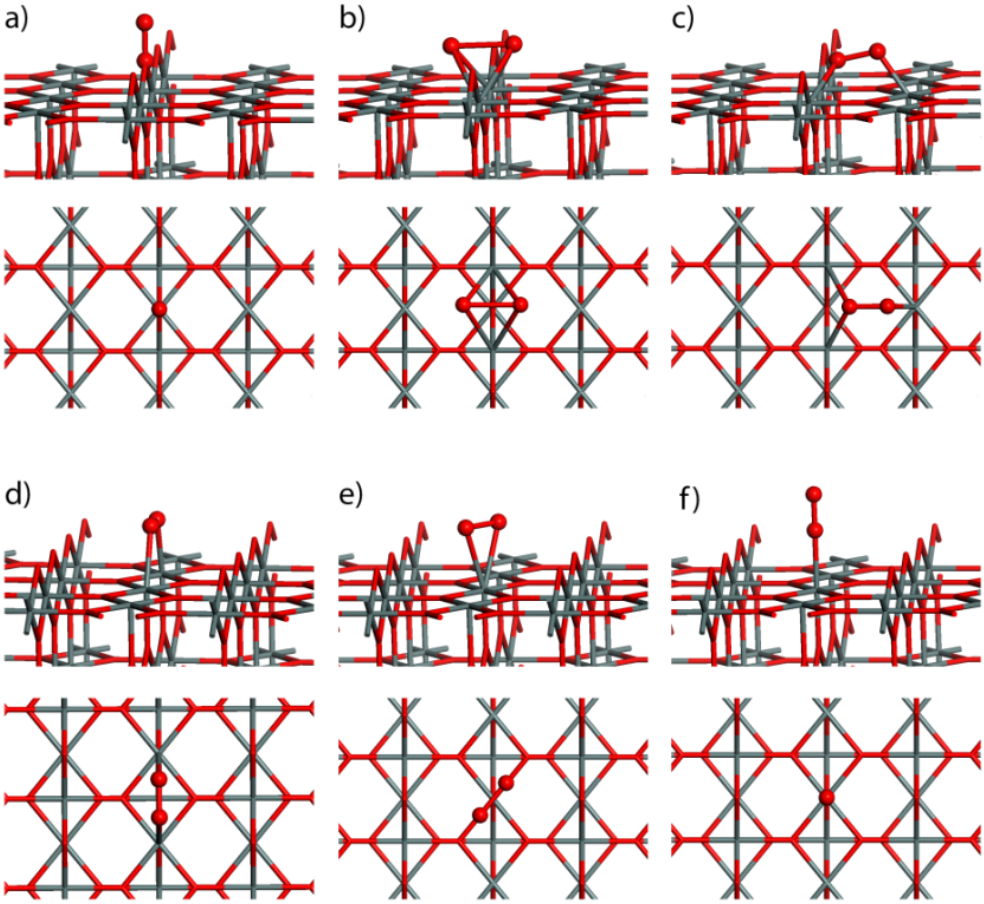

Figure 1. The side and top views of the molecular oxygen adsorption structures adsorbed at SnO_2 (110) surface. Sn and O atoms of the slab are represented as gray and red sticks, respectively, while adsorbed O atoms are represented as red spheres.

Table 1

Summary of the results from calculations of O_2 adsorbed at Sn_{5c} through in a parallel orientation.

Supercell with:	i) F_O impurity					ii) O_{br} vacancy			iii) F_O+O_{br}	iv) extra e^-	
Number of defects	1	2	3	4	6	1	2	3	1+1	"-1"	"-2"
Binding energy, (eV)	0.19	0.27	0.41	0.56	0.81	0.43	0.61	0.62	0.59	0.41	0.58
Length of O_2 bond (Å)	1.31	1.32	1.32	1.32	1.32	1.32	1.33	1.36	1.32	1.32	1.33
Spin density for O_2 (μ_B)	0.99	1.00	1.02	1.02	1.04	1.00	1.00	0.82	0.98	1.00	1.01
Spin density for O_{br} (μ_B)	0.20	0.14	0.10	0.05	0.00	0.25	0.01	0.00	0.01	0.04	0.00

The most prominent surface relaxation associated with such conformation is a downward displacement (0.55 Å) of the nearest to adsorbed O_2 molecule surface in-plane oxygen atoms. From the partial density of states (PDOS) projected on the adsorbed O_2^- we find that molecular π_g^* Kohn-Sham levels lie above the E_V, thus suggesting the existence of an acceptor level in the SnO_2 energy gap. The perpendicular to the surface π_g^* orbital ($\pi_g^{\perp}$) is fully occupied, while the parallel to the surface π_g^* orbital ($\pi_g^{\parallel}$) is filled for only spin-up electron, thus exhibiting spin polarization. The charge transfer to the $\pi_g^{\parallel}$ antibonding O_2 orbital is confirmed by similar isosurfaces of the spin density distribution shown in Figure 2 and the highest occupied molecular

orbital (HOMO) of O_2, which electron cloud is perpendicular to the axis of oxygen molecule. In abundance of surface free carriers the charge transfer from the substrate quenches the spin density of adsorbate to ~1.0 μ_B, which is half of the magnetic moment possessed by gas-phase O_2. The O–O bond of the parallel precursor is lengthened up to about 7% of the gas-phase O_2 bond length. These results indicate that the oxygen molecule is adsorbed through a chemisorption mechanism in superoxo-like form (O_2^-).

The lack of surface charge however has strong impact on the value of the calculated binding energy for adsorbed oxygen molecule. Earlier we have demonstrated that substitutional fluorine donor provides an extra charge to the crystal, which is delocalized in the perfect bulk [26,27]. The Bader charge analysis indicates that F_O donates to the conduction band only a fraction of the electron (0.33e). Approximately 0.66e is localized at F_O defect, deep in the band gap, and such electron density is not affected neither by O_2 adsorption nor by calculations of the host with one hole (q=+1). Thus more than one fluorine defect is needed to firmly stabilize superoxide at SnO_2 surface. Furthermore, the interaction of tin dioxide with oxygen molecule adsorbed in selected configuration apparently has electronic and magnetic components, which are strongly depending on the amount of excess electrons.

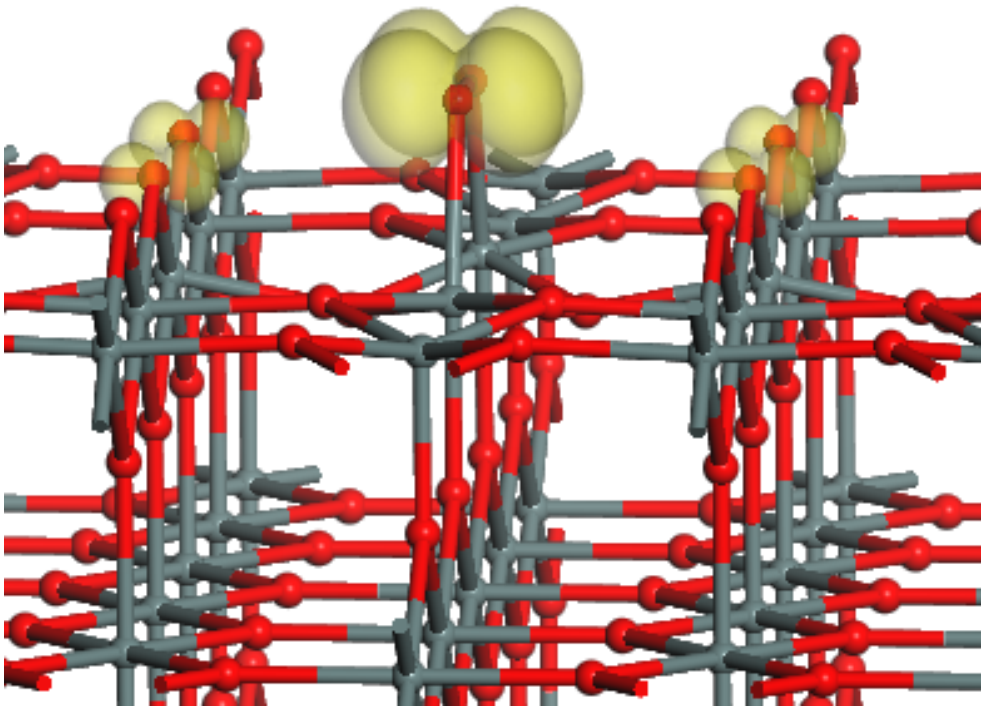

Figure 2. Isosurface of spin density distribution (contoured at 0.05 e Å^{-3}) for superoxide O_2^- molecule adsorbed at Sn_{5c} trough.

From the density difference plot (not shown) we deduce that neutral O_2 molecule placed above the five-fold tin sites on the perfect stoichiometric slab acquires fractional charge on its HOMO from the substrate thus causing electron deficiency on the surrounding surface atoms. This leads to induction of magnetic moments on the nearest to adsorbate O_{br} atoms and ferromagnetic coupling between them and O_2 as illustrated in Figure 2. Such oxygen molecule at stoichiometric (110) surface is metastable with endothermic energy of 0.4 eV. In slab with electron donors (F_O or O_{br} vacancies), the chemisorbed oxygen molecule withdraws one electron from SnO_2 substrate on its antibonding π_g^{II} orbital, which is at resonance with the Fermi level. However, in systems featured by the lack of surface electronic charge, like supercell doped with single fluorine atom, a weak magnetic coupling between O_2^- and neighboring O_{br} atoms is still observed. This

magnetic interaction destabilizes superoxide at SnO_2 (110) surface and eventually reduces its adsorption energy. As follows from the results summarized in Table 1, an accumulation of the surface surplus charge quenches spins on the O_{br} atoms and accordingly gives rise to E_b of the adsorbate. In other words, even if O_2 molecule has already accepted one electron from the substrate, more charge is needed for quenching the magnetic interaction and further stabilization of the adsorbate. The obtained results can be rationalized assuming that adsorbed O_2 molecule breaks stoichiometry of the slab and can be considered in reality as a surface fractional cation vacancy, which according to our recent results [28] can induce magnetism in the nearest oxygen atoms.

In principle, the electronic charge acquired by adsorbate can be donated by donor-type defects having different transition energy levels in the band gap, like bulk and surface oxygen vacancies or fluorine and hydrogen impurities. The relative positions of the local energy levels corresponding to the chemisorbed O_2 molecule and the main charge donors implicated in the calculations may affect the evaluation of the E_b. Indeed, an electronic charge donated by F_O impurity is delocalized in the conduction band, while bridging oxygen vacancies form the surface states that trap electrons about 0.7 eV below the E_C [1]. Accordingly, after desorption of O_2 molecule, the electron previously trapped at adsorbate is delocalized in the conduction band in the supercell with F_O, but is localized at O_{br} vacancy on reduced SnO_2 surface. The calculated E_b based on the total energy difference therefore should be higher in the former case, where additional charge is generated by the shallower donor-type defects. This constitutes an ambiguity in calculation of the O_2 binding energy, which depends on the origin of the electronic charge provided by the different donor-type defects mediating adsorption of O_2 molecule.

The saturation in the values of E_b with increased number of O_{br} vacancies in the supercell reflects the fact that the electron density remained after removing of the oxygen atoms is mainly localized at the vacancy sites. Mulliken population analysis indicates however that certain fraction of the electronic charge populates the surface Sn_{5c} that constitute E_C due to broadened occupation numbers with Gaussian-like smearing (width of 0.1 eV). This can explain close values of the binding energy calculated for the slabs, where sufficient additional charge is provided by four fluorine impurities (0.59 eV) or two O_{br} vacancies (0.61 eV). On the other hand, we find that Fermi level is profoundly shifted to the conduction band in the slab with six fluorine dopants thus giving unreasonable rise to the E_b. Based on the results summarized in Table 1, the correct value of the binding energy for O_2 molecule is estimated around 0.6 eV. Remarkably, the activation energies experimentally calculated on SnO_2 films from Arrhenius plots measured in different oxygen partial pressure are ranged from 0.56 to 0.65 eV in the temperature intervals corresponding to the stimulated desorption of oxygen species from the samples [29].

The transition state O_2^0/O_2^- calculated with PBE functional is found deep in the band gap (E_V+0.33 eV). This result corroborates findings of Bonapasta *et al* [30], based on the thermodynamic DFT approach and the same PBE functional. For O_2 molecule adsorbed at Ti^{+4} sites of (100) TiO_2 anatase surface they found transition energy level at E_V+0.29 eV. Such a deep position of the charge transition state for O_2 molecule would imply a high barrier to desorption. It is at variance both with E_b determined above from the total energy difference and with experimental observations. These discrepancies can be obviously related to the underestimation of the band gap in thermodynamic DFT approach based on PBE functional. In order to validate E_b values obtained at GGA-PBE level, we have performed the band gap corrected calculations with hybrid PBE0 functional for the supercells featured by the presence of one and two O_{br} vacancies. The calculated thus binding energies based on total energy differences (0.61 and 0.64 eV, respectively) are in line with our previous findings for the systems featured by abundance of the surface electronic charge.

3.2. Finite temperature effects

Accounting the adsorbate motion provides a complementary insight into the thermally stimulated desorption of O_2 precursors from SnO_2 surface. Since the experimental desorption times of $SnO_2 \cdots O_2$ system are longer than the simulation time scales accessible to the most efficient *ab initio* molecular dynamics schemes, we prepare the snapshot configurations by introducing small displacements of the oxygen atoms in adsorbed O_2 molecule in both positive and negative directions from their equilibrium positions and calculate the change in total energy versus offset using the static DFT approach. In the case of O_2 molecule lying parallel to the surface, the O–O bond length and the distance of O_2 center of mass from the fixed centermost atomic layer are chosen as the reaction coordinates in determination of the desorption pathway. Thermally stimulated desorption of molecular oxygen is explored first on the allowed to relax surface with fixed equilibrium lattice constants. The effect of surface strain is then investigated by compressed or stretched lattice constants, whereon various properties are calculated again.

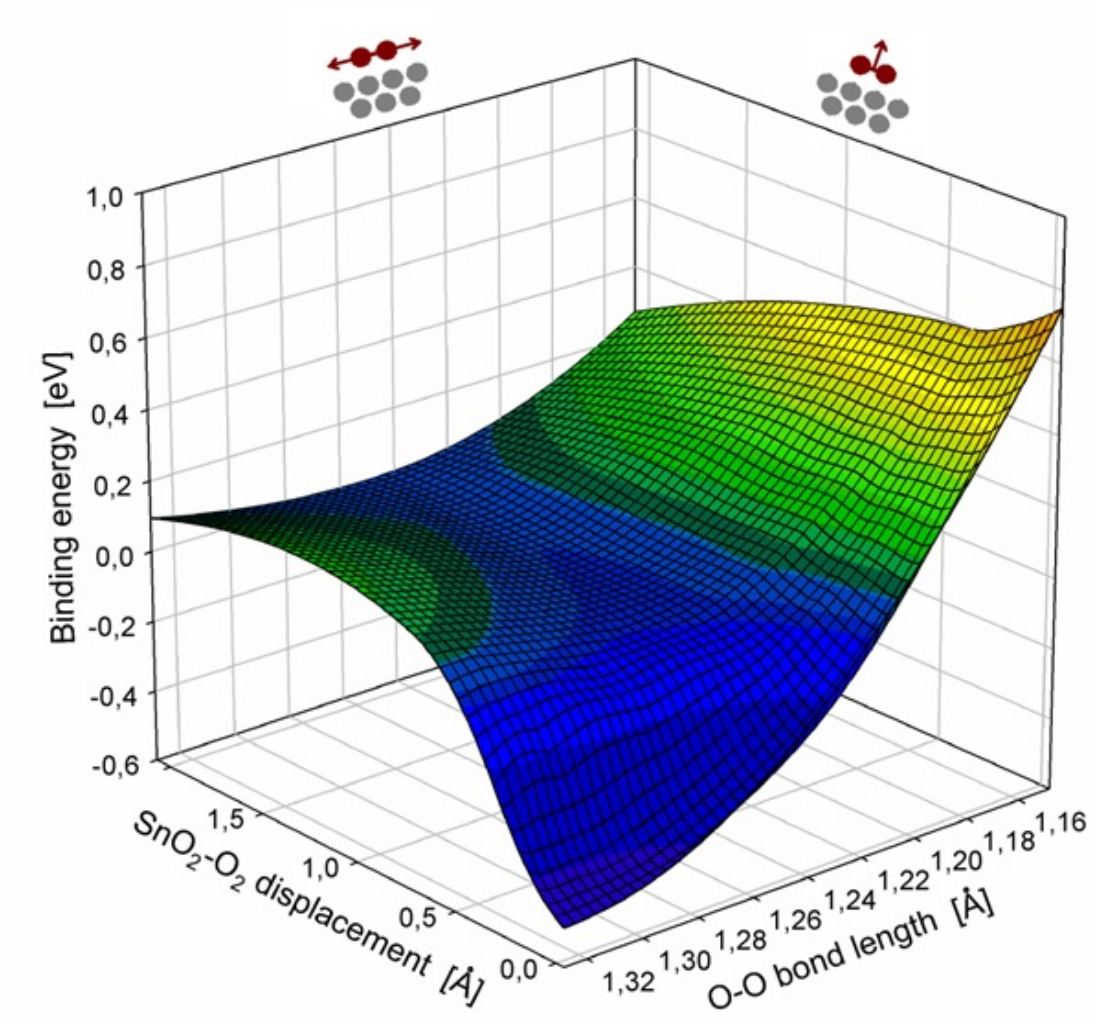

Figure 3. The calculated potential-energy surface representing the binding energy of oxygen molecule adsorbed at the SnO_2 Sn_{5c} through as a biaxial function of O–O bond length and displacement of O_2^- center of mass from its optimized position, induced by vibration modes.

The calculated binding energy for O_2 adsorbed at the SnO_2 surface as a biaxial function of SnO_2–O_2 and internal O–O vibration modes is presented in Figure 3. The change in energy versus variable position results in a potential-energy surface, from which we determine the O–O stretching frequency and desorption frequency factor (ν) using the harmonic oscillator

approximation. The vibrational frequency belonging to the O–O stretching mode is red-shifted with respect to free O_2 molecule (1580 cm^{-1}) and is found to be 1140 cm^{-1}. This is in good agreement with experimentally measured vibration frequencies of O_2^- adsorbed on SnO_2 surface (1045 cm^{-1} and 1190 cm^{-1}) [31]. The critical displacement at which O_2^- is discharging upon lifting from the surface amounts approximately to 0.4 Å as traced by Mulliken population analysis. In this transition state the magnetic moment of oxygen molecule increases from ~1.0 μ_B to 2.0 μ_B, which is characteristic of the gas phase O_2 molecule in triplet state. Before that the binding energy is increasing with distance by quadratic law. The calculated value of v is therefore estimated as 2×10^{11} s^{-1}, which is few orders of magnitude lower than the frequency factor (10^{13} s^{-1}) provided by the classical Eyring's theory [32], but higher than values 2×10^{8}–3×10^{9} s^{-1}, obtained for $SnO_2\cdots O_2$ system in TPD experiments [33]. These differences illustrate some limitations of the TPD methods based on peak maximum temperatures and described elsewhere [33,34]. On the other hand, it is known that GGA-PBE calculations overestimate the vibrational frequencies by several percent [35].

The phenomenological treatment of individual and collective effects of adsorbate on the transducer function of semiconductor sensor has been reported by us elsewhere [36]. In framework of the Volkenstein model [37], the thermal activation of an electron from the chemisorption state into the conduction band (in the case of an acceptor-type surface defect) is considered as the precursor for desorption of the neutral molecule, since lifetime in the physisorbed state is assumed to be negligible. By contrast, the time-dependent DFT approach applied recently for TiO_2–O_2 system [38] predicts the lifetime of excited O_2 molecule (i.e. state, in which an electron trapped by adsorbed O_2 molecule is injected back into the substrate) to be 266 fs. The calculated lifetime is short enough as compared with characteristic time of the O_2 precursor (5 ps) evaluated from the pre-exponential frequency factor (v) that points out on the high probability of readsorption, which may occur in case if excess electronic charge is available at the surface. This option is not taken into account in TPD measurements based on peak maximum temperatures.

The readsorption occurs effectively when free electron carriers are available on the surface, e.g. for SnO_2 doped with fluorine impurity. With F_O defects as the main charge donors the additional charge is delocalized in the conduction band and can be readily retrapped by excited O_2 molecule. While O_{br} vacancies also provide the surface excess electrons, the extra charge is mainly localized around the defects. Being a surface trapping centers, the bridging oxygen vacancies can capture electrons released by oxygen species thus reducing the probability of O_2 readsorption.

Analysis of Figure 3 indicates that contribution of the O–O stretching mode to decrease of the adsorption barrier is approximately twice lower than that of the center-of-mass (SnO_2–O_2) mode. The 5% compression of the O–O bond leads to reducing of the E_b on 0.16 eV, while 5% displacement of the O_2 center of mass from its optimal position on the SnO_2 surface is accompanied by diminishing of the adsorption barrier on 0.3 eV. Such behavior implies that coupling between the p-orbitals of oxygen molecule is less sensitive to the thermal motion than $\pi_g^{\perp}$ hybrid formed between p-orbital of O_2 molecule and s-orbital of the surface Sn_{5c} atom, apparently because of the more delocalized character of Sn s-states in s-p hybrid as compared with anion p states, where directional bonding plays significant role.

When oxygen molecule vibrates on the surface, the position of the π_g^* resonances relative to the ε_F also oscillates, which would mean also a large fluctuation in the occupation numbers of the π_g^* orbitals. The calculated shifts of the O_2^- $\pi_g^{\parallel}$ HOMO and the $\pi_g^{\perp}$ hybrid orbital as a function of dynamic snapshots for different fully relaxed adsorbate-surface conformations upon lifting of

the O_2^- from its equilibrium position are presented in Table 2. The internal stretching vibrations of the O_2 molecule are reflected in strong (~3 eV) fluctuation of its antibonding π_g^{II} and $\pi_g^{\perp}$ Kohn-Sham levels with respect to the deep $1\sigma_g$ orbital of the same molecule, while variation of the π_g^{II} resonance relative to the 5s orbitals of the Sn_{5c} surface sites is less pronounced and amount to 0.5 eV. As expected, the $\pi_g^{\perp}$ orbital exhibits the greatest upshift of 1.5 eV in response to displacement of the oxygen molecule, which points out on the significant local synergetic effect induced by the mutual vibration of the O_2^- and underneath Sn_{5c} surface atoms on the charge oscillations between the molecular $\pi_g^{\perp}$ resonance and the substrate.

Table 2

The calculated from PDOS shifts in energies (eV) of the $\pi_g^{\perp}$ hybrid orbital; the π_g^{II} HOMO and the π_g^{II} LUMO caused by the displacement of the center of mass (ΔR) of the chemisorbed O_2^- molecule from its optimal position on the SnO_2 surface. Positive values correspond to upshift in position of the orbital.

	Relative to the O_2 $1\sigma_g$-orbital		Relative to the Sn_{5c} 5s-orbitals	
ΔR, Å	$\pi_g^{\perp}$	π_g^{II} HOMO	$\pi_g^{\perp}$	π_g^{II} HOMO
0.1	0.10	0.14	0.18	0.21
0.2	0.18	0.23	0.28	0.32
0.3	0.85	0.96	0.53	0.43
0.4	1.90	1.80	0.92	0.48
0.5	2.72	2.65	1.18	0.53
0.6	2.90	2.85	1.39	0.55
0.7	3.05	2.92	1.52	0.52
0.8	3.10	2.99	1.54	0.49

In order to evaluate the effect of surface strain on the thermochemistry of O_2 desorption we used lattice constants 2% less than the equilibrium values to model a compressed surface and 2% more than the equilibrium values to model a stretched surface. We find that surface contraction increases stability of O_2 adsorbate, while lattice expansion implies a lower barrier to desorption due to the lower binding energy of O_2 with Sn_{5c} surface sites. The surface stretching of 2% leads to E_b of only 0.05 eV, while the trapped electron is still found on the oxygen molecule. The further injection of the electron into the conduction band induced by the thermally stimulated adsorbate-surface motion has very high probability.

The corresponding PDOS reflecting the effect of surface strain are presented in Figure 4. The surface expansion of 2% causes downshift (0.5 eV) of the Sn 5s-orbitals, while all π_g^* levels of the chemisorbed O_2^- molecule move slightly upward (0.06 eV). Surface compression of 2% leads to increase in energy of the Sn s-orbitals on 0.4 eV. The $\pi_g^{\perp}$ and the π_g^{II} HOMO behaves similarly and move down in the band gap on 0.47 eV, while π_g^{II} LUMO is shifting down on only 0.06 eV. The strong variation of the Sn edge states induced by the thermal expansion corroborates results of Li *et al* [39], where by applying a small isotropic strain a changes of SnO_2 band gap as large as 0.8 to 1 eV are obtained. The similar downshift of the occupied $\pi_g^{\perp}$ and π_g^{II} orbital levels induced by the surface contraction reflects the stabilization of the adsorbate due to stronger ionic bonding with surface [40]. The coupling of the π_g^{II} LUMO with Sn 5s-orbitals constituting the E_C upon surface expansion indicates that in abundance of the surface free carriers, the desorption of O_2 molecule can be additionally stimulated by capturing of an extra electron on its antibonding π_g^{II} orbital.

The surface quasiharmonic (volumetric) contribution to the O_2 desorption pathway dominates the effect arise from the thermal motion associated with the center-of-mass (SnO_2–O_2) mode, which is in turn twice stronger than the effect of the O–O internal stretching mode. The aggregate fluctuation of the π_g^* resonances due to thermal broadening and mutual vibrations of O_2 molecule and surface can reach 1 eV. This value is comparable with calculated adsorption energy (0.6 eV) of O_2 molecule, which implies lowering or even vanishing of the activation

barrier to desorption at finite temperatures. Accounting the vibrational contributions can provide insight into the low-temperature (below 200 K) desorption of O_2 molecules from SnO_2 surface, notwithstanding the adsorption energy of oxygen species is noticeable.

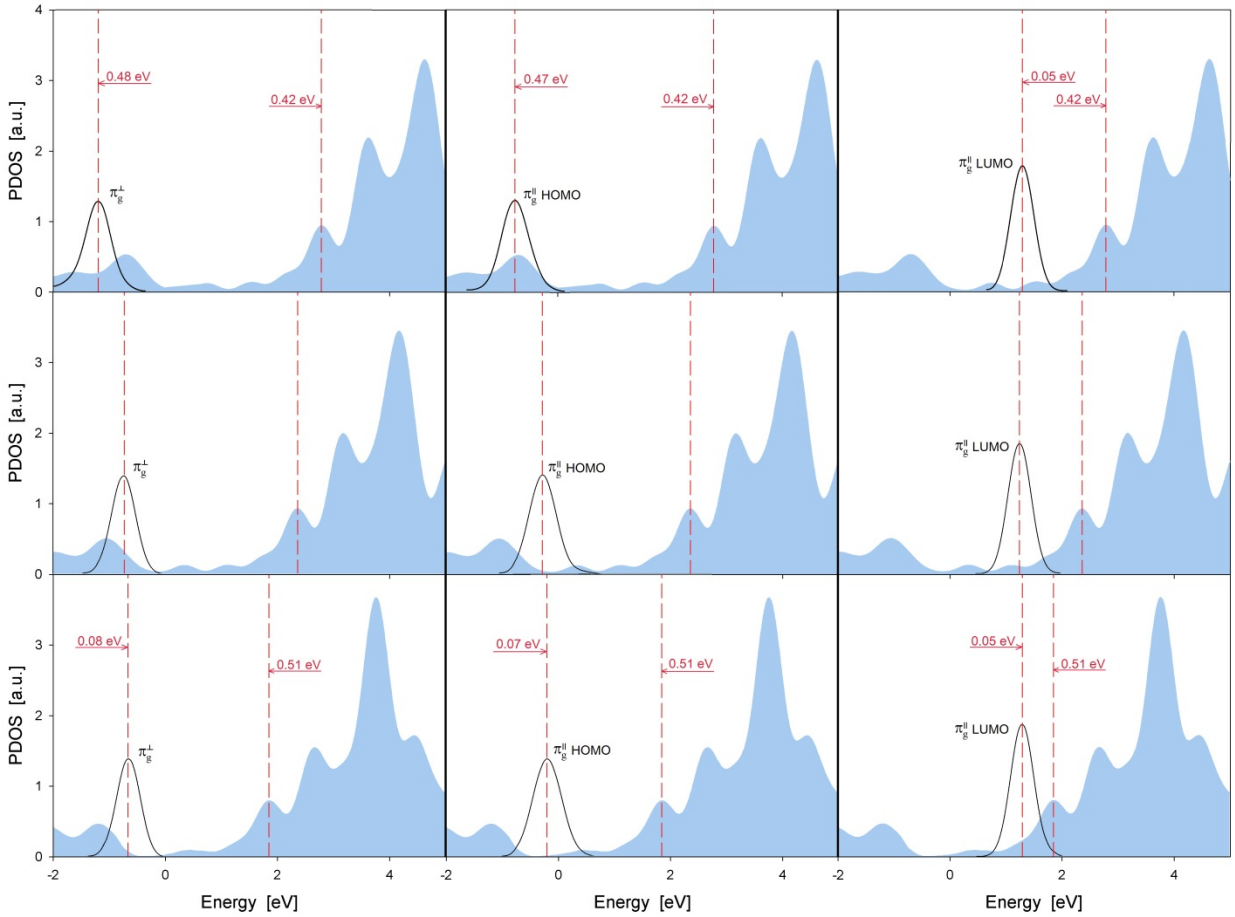

Figure 4. The PDOS of the Sn_{5c} surface atoms (blue area) and the PDOS of the $\pi_g^{\perp}$ hybrid orbital (left panel); the $\pi_g^{\parallel}$ HOMO (center panel) and the $\pi_g^{\parallel}$ LUMO (right panel) of the O_2^- molecule adsorbed on-top of the Sn_{5c} surface atoms (black line) calculated for a) compressed by 2% surface, b) surface with equilibrium lattice constants, and c) surface stretched by 2%. The red arrows indicate direction and values of the shifts in the energetic position of the corresponding orbitals.

The transfer of electrons from ionosorbed analyte to empty electron states inside the adsorbent solid is the key reaction in the surface ionization experiments [41,42], where ionized analyte species are extracted into a free space by a counter electrode positioned at a short distance above the hot emitter surface. As usual, the counter electrode is negatively biased to observe positive ion emission from SnO_2. Accordingly, authors did not observe an ion current associated with presence of the O_2^+ ions that can be connected with high ionization energy of the molecular oxygen species. On the other hand, our calculations predict substantial decreasing of the energy needed to detach O_2^- radical from the SnO_2 (110) surface enriched by negative surplus charge comparing to 4.5 eV necessary to detach O_2^- radical from the perfect neutral surface. Thus, experiments with adsorbed oxygen species and positively biased counter electrode for SnO_2 with high concentration of the free carriers achieved by heavy doping would be very promising.

4. Conclusions

In summary, we find that oxygen molecule is adsorbed in superoxide-like form (O_2^-) on top of the five-coordinated surface tin atoms. The binding energy of adsorbate strongly depends on the

availability of free carriers. At lack of surface electronic charge, the oxygen molecule induces magnetic moments on the nearest O_{br} atoms, which eventually destabilize superoxide at SnO_2 (110) surface. In abundance of surplus electrons the adsorption energy of O_2 molecule is estimated to be about 0.6 eV. Such species can be therefore associated with low-temperature (<200 K) peak observed in the TPD experiments.

We demonstrate that the nature of the main charge donors implicated in the calculations, in particular, the position of their transition levels with respect to the local energy level corresponding to adsorbed molecule have influence on the evaluation of the adsorption energy. The finite temperature effects associated with the adsorbate-surface motions have a strong impact on position of the antibonding π_g^* levels of the O_2^- molecule with respect to the ε_F in SnO_2. The calculated thermally driven fluctuations are comparable with adsorption energy of the O_2 molecule, which can explain the low-temperature desorption of the O_2 molecule from SnO_2 surface.

By comparison of the characteristic time for adsorbed O_2 precursor with the lifetime of oxygen molecule in excited state we deduce that the surface electronic charge has influence on the parameters of desorption through the readsorption channel. In other words, at lack of the electronic charge, the relatively slow thermally activated bond breaking processes (as compared to fast recharging) are the bottleneck for O_2 desorption. This is at variance with well-known Volkenstein model, where electronic processes, and in particular, position of the ε_F in the band gap always dominates the kinetics of thermal desorption. It can be concluded that doping with shallow donor-type defects, like fluorine or hydrogen, which leads to enrichment of the surface with excess charge, can substantially hinder the rate of molecular oxygen desorption.

We could draw the picture that describes the molecular oxygen desorption path as following. At high temperatures in oxygen-rich limit, which is actually a favorable operation regime for the SnO_2-based chemical sensors, the oxygen atoms diffusing along the Sn_{5c} rows can recombine in weakly bound oxygen molecules, thus forming thermodynamically favorable precursors for the O_2 desorption pathway. This implies the second-order desorption kinetics rather than first-order kinetics observed in low-pressure TPD experiments performed under ultra-high vacuum conditions.

Acknowledgment

This work was partially supported by FP7-PEOPLE Marie Curie International Incoming Fellowship Program (project MOEBIUS). Computational resources were provided by the CSC — IT Center for Science, Espoo, Finland.

5. References

[1] M. Batzill, U. Diebold, The surface and materials science of tin oxide, *Progress of Surf. Sci.* 79 (2005) 45–154.

[2] J. Oviedo, M. Gillan, First-principles study of the interaction of oxygen with the SnO_2 (110) surface, *Surface Science* 490 (2001) 221-236.

[3] B. Slater, C. Catlow, D. Williams and A. Stoneham, Dissociation of O_2 on the reduced SnO_2 (110) surface, *Chem. Commun.*, (2000) 1235–1236.

[4] F. Sensato, R Custodio, M. Calatayud, A. Beltran, J. Andres, J. Sambrano, E. Longo, Periodic study on the structural and electronic properties of bulk, oxidized and reduced SnO_2 (110) surfaces and the interaction with O_2, *Surface Science* 511 (2002) 408–420.

[5] M. Habgood, N. Harrison, An ab initio study of oxygen adsorption on tin dioxide, *Surface Science* 602 (2008) 1072–1079.
[6] M. Viitala, O. Cramariuc, T.T. Rantala, V. Golovanov, Small hydrocarbon adsorbates on SnO_2 (110) surfaces: Density functional theory study, *Surface Science* 602 (2008) 3038–3042.
[7] E. Lira, P. Huoa, J. Hansen, F. Rieboldta, R. Bechsteina, Y. Wei, R. Strebera, S. Porsgaard, Z. Li, E. Lægsgaard, S. Wendt, F. Besenbacher, Effects of the crystal reduction state on the interaction of oxygen with rutile TiO_2 (110), *Catalysis Today* 182 (2012) 25– 38.
[8] E. Lira, J. Hansen, P. Huo, R. Bechstein, P. Galliker, E. Lægsgaard, B. Hammer, S. Wendt, F. Besenbacher, Dissociative and molecular oxygen chemisorption channels on reduced rutile TiO_2 (110): An STM and TPD study, *Surface Science* 604 (2010) 1945–1960.
[9] M. Henderson, W. Epling, C. Perkins, C. Peden, U. Diebold, Interaction of molecular oxygen with the vacuum-annealed TiO_2 (110) surface: molecular and dissociative channels, *J. Phys. Chem.* B 103 (1999) 5328-5337.
[10] M. Mäki-Jaskari, T. T. Rantala, V. Golovanov, Computational study of charge accumulation at SnO_2 (110) surface, *Surface Science* 577 (2005) 127–138.
[11] V. Milman, B. Winkler, J.A. White, C.J. Pickard, M.C., Payne, E.V. Akhmatskaya, R.H. Nobes, Electronic structure, properties, and phase stability of inorganic crystals: A pseudopotential plane-wave study, *Int. J. Quant. Chem.* 77 (2000) 895-910.
[12] D. Vanderbilt, Soft self-consistent pseudopotentials in generalized eigenvalue formalism, *Phys. Rev. B* 41 (1990) 7892-7895.
[13] J. P. Perdew, J. A. Chevary, S. H. Vosko, K. A. Jackson, M. R., Pederson, D. J. Singh, and C. Fiolhais, Atoms, molecules, solids, and surfaces: Applications of the generalized gradient approximation for exchange and correlation, *Phys. Rev. B* 46 (1992) 6671–6687.
[14] M. Marsman, J. Paier, A. Stroppa and G. Kresse G, Hybrid functionals applied to extended systems, *J. Phys.: Condens. Matter* 20 (2008) 064201.
[15] P. Blöchl, Projector augmented-wave method, *Phys. Rev. B* 50 (1994) 17953–17979.
[16] P. Agoston, K. Albe, R. Nieminen, and M. Puska, Intrinsic *n*-type behavior in transparent conducting oxides: A comparative hybrid-functional study of In_2O_3, SnO_2, and ZnO, *Phys. Rev. Lett*. 103 (2009) 245501-4.
[17] C. Freysoldt, J. Neugebauer, C.G. Van deWalle, Fully ab initio finite-size corrections for charged-defect supercell calculations, *Phys. Rev. Lett*. 102 (2009) 016402.
[18] U. Pulkkinen, T. T. Rantala, T. S. Rantala, V. Lantto, Kinetic Monte Carlo simulation of oxygen exchange of SnO_2 surface, *J. Mol. Catal. A:* C 166 (2001) 15–21.
[19] A. Tilocca and A. Selloni, O_2 and vacancy diffusion on rutile (110): pathways and electronic properties, *Chem. Phys. Chem*. 6 (2005) 1911 – 1916.
[20] N. Zhanpeisov and H. Fukumura, Oxygen vacancy formation on rutile TiO_2 (110) and its interaction with molecular oxygen: A theoretical density functional theory study, *J. Phys. Chem.* C 111 (2007) 16941-16945.
[21] M. D. Rasmussen, L. M. Molina, and B. Hammer, Adsorption, diffusion, and dissociation of molecular oxygen at defected TiO_2 (110): A density functional theory study, *J. Chem. Phys*., 120(2) (2004) 988-997.
[22] H. Xu, S.Y. Tong, Interaction of O_2 with reduced rutile TiO_2 (110) surface, *Surface Science* 610 (2013) 33–41.
[23] M.P. de Lara-Castells, J. Krause, Theoretical study of the interaction of molecular oxygen with a reduced TiO_2 surface, *Chemical Physics Letters* 354 (2002) 483–490.
[24] C. Shu, N. Sukumar, and C. Ursenbach, Adsorption of O_2 on TiO_2 (110): A theoretical study, *J. Chem. Phys.*, 110(21) (1999) 10539-10544.
[25] E. Wahlstrom, E. Vestergaard, R. Schaub, A. Ronnau, M. Vestergaard, E. Lægsgaard, I. Stensgaard, F. Besenbacher, Electron transfer–induced dynamics of oxygen molecules on the TiO_2 (110) surface, *Science* 303 (2004) 511-513.

[26] N. Őzcan, T. Kortelainen, V. Golovanov, T. T. Rantala, and J. Vaara, Electron spin resonance parameters of bulk oxygen vacancy in semiconducting tin dioxide, *Phys. Rev*. *B* 81 (2010) 235202-10.

[27] V. Golovanov, M. Viitala, T. Kortelainen, O. Cramariuc, T. Rantala, Stability of siloxane couplers on pure and fluorine doped SnO_2 (110) surface: A first principles study, *Surface Science* 604 (2010) 1784–1790.

[28] V. Golovanov, V. Golovanova, M. Kuisma and T. T. Rantala, Electron spin resonance parameters of cation vacancies in tin dioxide doped with fluorine and hydrogen, *Journal of Applied Physics*, 114 (2013) 143907.

[29] V. Lantto and V. Golovanov, A comparison of conductance behavior between SnO_2 and CdS gas-sensitive films, *Sensors and Actuators* B 24-25 (1995) 614-618.

[30] A. Bonapasta and F. Filippone, Photocatalytic reduction of oxygen molecules at the (100) TiO_2 anatase surface, *Surface Science* 577 (2005) 59-68).

[31] T.A. Gundrizer, A.A. Davydov, Infrared spectra of oxygen adsorbed on SnO_2, *React. Kinet. Catal. Lett*. 3 (1975) 67-70.

[32] R.I. Masel, Principles of adsorption and reaction on solid surfaces, John Wiley & Sons, New York, 1996.

[33] D. Puzzovio, M.C. Carotta, A. Cervi, A. El Hachimi, J.P. Joly, F. Gaillard, V. Guidi, TPD and ITPD study of materials used as chemoresistive gas sensors, *Solid State Ionics* 180 (2009) 1545–1552.

[34] J. Niemantsverdriet, K. Wandelt, The compensation effect in thermal desorption of adsorbate systems with lateral interactions, *J. Vac. Sci. Technol*., A6(3) (1988) 757-761.

[35] A. Scott and L. Radom, Harmonic vibrational frequencies: An evaluation of Hartree−Fock, Møller−Plesset, quadratic configuration interaction, density functional theory, and semiempirical scale factors, *J. Phys. Chem*., 100(41) (1996) 16502-16513.

[36] V. Golovanov and V. Smyntyna, Interaction between collective and local subsystems in semiconductor surface-active structures, *Sensors and Actuators* B 24-25 (1995) 647-652.

[37] F. Volkenstein, Electronic processes on semiconductor surfaces during chemisorption, Consultants Bureau, New York, 1991.

[38] P. Dholabhai and H. Yu, Electronic structure and quantum dynamics of photoinitiated dissociation of O_2 on rutile TiO_2 nanocluster, *J. Chem. Phys*. 138 (2013) 194705-12.

[39] H. Li, I. Castelli, K. Thygesen, and K. Jacobsen, Strain sensitivity of band gaps of Sn-containing semiconductors, *Phys. Rev.* B 91 (2015) 045204-6.

[40] M. Viitala, O. Cramariuc, T. Rantala, V. Golovanov, Small hydrocarbon adsorbates on SnO_2 (110) surfaces: Density functional theory study, *Surface Science* 602 (2008) 3038–3042.

[41] A. Hackner, A. Habauzit, G. Muller, Resistive and surface ionization response of SnO_2 gas sensing layers, *Sensors and Actuators* B 146 (2010) 433–439.

[42] C. Oberhuttinger, A. Hackner, G. Muller, M. Stutzmann, On the temperature dependence of the resistive and surface ionization response of SnO_2 gas sensing layers, *Sensors and Actuators* B 156 (2011) 563– 571.